

# Evidence that the maximum electron energy in hotspots of FR II galaxies is not determined by synchrotron cooling

Anabella T. Araudo,<sup>1\*</sup> Anthony R. Bell,<sup>2</sup> Aidan Crilly<sup>1,3</sup> and Katherine M. Blundell<sup>1</sup>

<sup>1</sup>University of Oxford, Astrophysics, Keble Road, Oxford OX1 3RH, UK

<sup>2</sup>University of Oxford, Clarendon Laboratory, Parks Road, Oxford OX1 3PU, UK

<sup>3</sup>University of Cambridge, Downing College, Regent Street, Cambridge CB2 1DQ, UK

Accepted XXX. Received YYY; in original form ZZZ

## ABSTRACT

It has been suggested that relativistic shocks in extragalactic sources may accelerate the highest energy cosmic rays. The maximum energy to which cosmic rays can be accelerated depends on the structure of magnetic turbulence near the shock but recent theoretical advances indicate that relativistic shocks are probably unable to accelerate particles to energies much larger than a PeV. We study the hotspots of powerful radiogalaxies, where electrons accelerated at the termination shock emit synchrotron radiation. The turnover of the synchrotron spectrum is typically observed between infrared and optical frequencies, indicating that the maximum energy of non-thermal electrons accelerated at the shock is  $\lesssim$  TeV for a canonical magnetic field of  $\sim 100 \mu\text{G}$ . Based on theoretical considerations we show that this maximum energy cannot be constrained by synchrotron losses as usually assumed, unless the jet density is unreasonably large and most of the jet upstream energy goes to non-thermal particles. We test this result by considering a sample of hotspots observed with high spatial resolution at radio, infrared and optical wavelengths.

**Key words:** galaxies: active – galaxies: jets – acceleration of particles – radiation mechanisms: non-thermal – shock waves

## 1 INTRODUCTION

Active Galactic Nuclei (AGN) have been proposed as sources of Ultra High Energy Cosmic Rays (UHECRs). Shocks with different velocities and extents are present in jets of Fanaroff-Riley (FR) radiogalaxies (Fanaroff & Riley 1974), where particles can be accelerated via diffusive shock acceleration. In particular, relativistic and mildly relativistic shocks with velocity  $v_{\text{sh}}$  at the jet termination region might accelerate particles with Larmor radius  $r_g \sim R_j$ , where  $R_j \sim 1$  kpc is the jet width. Particles with such a large  $r_g$  in a magnetic field  $\sim 100 \mu\text{G}$  have energy

$$\frac{E_{\text{UHECR}}}{\text{EeV}} \sim 100 \left( \frac{v_{\text{sh}}}{c/3} \right) \left( \frac{B}{100 \mu\text{G}} \right) \left( \frac{R_j}{\text{kpc}} \right), \quad (1)$$

as expected for UHECRs (Lagage & Cesarsky 1983; Hillas 1984). In particular, Rachen & Biermann (1993) and Norman et al. (1995) concluded that hotspots of FR II radiogalaxies are plausible sources of UHECRs (see also Nagano & Watson 2000; Kotera & Olinto 2011). But, there are two assumptions behind Eq. (1): 1) particles diffuse in the Bohm regime, i.e. the mean-free path is  $\lambda \sim r_g$ , and 2) the mag-

netic field  $B$  persists over distances  $\sim R_j$  downstream of the shock.

Protons are the dominant component of UHECRs. Given that ion radiation losses are slow in low density plasmas such as AGN jets, protons can be accelerated up to energies  $E_{p,\text{max}} \sim E_{\text{UHECR}}$  if both assumptions are satisfied. However, there are no hadronic radiative signatures from hotspots and therefore we do not have any observational information about  $E_{p,\text{max}}$ . In consequence, we investigate the validity of assumptions 1) and 2) by modelling the synchrotron emission produced by non-thermal electrons accelerated at the jet reverse shock. The synchrotron turnover at  $\nu_c \gtrsim 10^{14}$  Hz typically observed in hotspots of FR II galaxies (e.g. Meisenheimer & Heavens 1986; Meisenheimer et al. 1997; Tavecchio et al. 2005; Stawarz et al. 2007; Werner et al. 2012) indicates that the maximum energy of non-thermal electrons is

$$\frac{E_c}{\text{TeV}} \sim 0.2 \left( \frac{\nu_c}{10^{14} \text{ Hz}} \right)^{\frac{1}{2}} \left( \frac{B}{100 \mu\text{G}} \right)^{-\frac{1}{2}} \quad (2)$$

(Ginzburg & Syrovatskii 1964), much smaller than  $E_{\text{UHECR}}$  for reasonable values of the magnetic field. The traditional assumption is that  $E_c$  is determined by synchrotron cooling and therefore the diffusion coefficient of particles with such

\* E-mail: Anabella.Araudo@physics.ox.ac.uk

an energy is

$$\frac{\mathcal{D}_{c,s}}{\mathcal{D}_{\text{Bohm}}} \sim 10^7 \left( \frac{v_{\text{sh}}}{c/3} \right)^2 \left( \frac{\nu_c}{10^{14} \text{ Hz}} \right)^{-1} \quad (3)$$

(e.g. Stage et al. 2006; Kirk & Reville 2010). Protons with energy  $\sim E_c$  also diffuse with  $\mathcal{D}_{c,s}$  and therefore the maximum energy that they can achieve is reduced to 10 TeV instead of 100 EeV as expected from the Hillas constraint in Eq. (1), assuming that  $B$  persists over distances larger than the synchrotron cooling length  $l_c$  of electrons with energy  $E_c$ . However, theoretical results of Weibel-mediated shocks (e.g. Spitkovsky 2008a), and observational analysis of the case study of 4C74.26 (Araudo et al. 2015) indicate that the magnetic field is damped in the downstream region of a relativistic shock.

Numerical simulations show that Weibel-mediated shocks in relativistic and weakly magnetised plasmas amplify the magnetic field on scale length  $s \ll r_g$ , where  $r_g$  is the Larmor radius of particles being accelerated (Spitkovsky 2008a,b). The mean-free path for scattering by small-scale turbulence ( $\lambda \sim r_g^2/s$ ) is larger than the size of the system ( $R_j$  in our case) if  $s$  is comparable with the plasma skin depth  $c/\omega_{\text{pi}}$  and  $r_g$  is the Larmor radius of an EeV proton. These small-scale magnetic fluctuations decay at a distance  $\sim 100 c/\omega_{\text{pi}}$  downstream of the shock, corresponding to  $\sim 10^{11}$  cm for a mildly relativistic plasma with density of the order of  $10^{-4} \text{ cm}^{-3}$  (see Eq. (14)). This rapid decay of the fluctuations inhibits particle acceleration to EeV energies, as was pointed out by Lemoine & Pelletier (2010); Sironi et al. (2013) and Reville & Bell (2014).

Damping of the magnetic field in the downstream region of a relativistic shock was observationally confirmed by modelling the jet termination region of the quasar 4C74.26 (Araudo et al. 2015). The compact synchrotron emission ( $\sim 0.1$  kpc) detected in the southern hotspot of this source would require a magnetic field  $\sim 2.4$  mG to match the size of the emitter with the synchrotron cooling length at the observed frequency of 1.66 GHz. This value of the magnetic field is about 10 times the upper limit imposed by the equipartition condition with non-thermal particles (see more details of the model in Araudo et al. (2016)). Therefore, the compact radio emission delineates the region within which the magnetic field is amplified by plasma instabilities up to  $\sim 100 \mu\text{G}$ , and it is damped downstream of the shock.

In Araudo et al. (2015) we consider the standard framework to explain the cut-off of the synchrotron spectrum at IR/optical frequencies and we discussed the thickness of the synchrotron emitter in the context of Weibel instabilities. Given that the thickness of the MERLIN radio emitter in the southern hotspot of 4C74.26 is larger than the synchrotron cooling length of  $E_c$ -electrons, we interpreted this behaviour of  $E_c$  being determined by synchrotron cooling, and then, at distances  $\sim 0.1$  kpc downstream of the shock, the magnetic field is damped as a consequence of the small scale of Weibel turbulence. However,  $\sim 0.1$  kpc is much larger than the turbulence decay length predicted by numerical simulations of Weibel-mediated shocks in plasmas with densities  $\sim 10^{-4} \text{ cm}^{-3}$ .

In the present work we carry out a deeper study of particle acceleration in the hotspots of FR II radiogalaxies. We revisit the assumption of the synchrotron turnover being determined by synchrotron losses. Given that the scale-length

of magnetic fluctuations has to be larger than  $c/\omega_{\text{pi}}$  (see Sect. 3), we show that  $E_c$  cannot be determined by synchrotron cooling, as usually assumed, unless the jet density is unreasonably large and most of the jet upstream energy goes to non-thermal particles. We also show that the Weibel instability is not the source of the amplified magnetic field throughout the whole hotspot emission region since not only does it damp too quickly, but also it generates turbulence on a very small scale, insufficient to accelerate particles up to  $E_c \sim \text{TeV}$  for typical values of the magnetic field. In Sect. 5 we discuss the alternative possibility that the magnetised turbulence is generated by the Non Resonant Hybrid instability (Bell 2004) which damps less quickly and grows on a larger scale.

In Table 1 we present some of the mathematical relations we use and how the reigning paradigm violates energy conservation even with very conservative assumptions. We consider the sample of hotspots observed with high spatial resolution at radio, infrared (IR) and optical frequencies in Mack et al. (2009). We find that very low values of the magnetic field, and therefore a huge energy density in non-thermal electrons, would be required to explain the flux density at 8.4 GHz if the IR/optical cut-off of the synchrotron spectrum was constrained by synchrotron cooling (see Sect. 3.1). These results invite the revision of previous phenomenological models of the hotspots non-thermal emission.

The results presented in this paper have also important implications for Eq. (1) and the maximum energy that protons can achieve by being accelerated in the jet reverse shock. We conclude that hotspots of FR II radiogalaxies with optical synchrotron cut-off are very poor accelerators of UHECRs.

The paper is organised as follows: In Sect. 2 we introduce the reader to state-of-the-art modelling of non-thermal particles in hotspots. In Sect. 3 we revise the assumption that the acceleration process ceases as a consequence of efficient synchrotron losses and show that this standard picture is in disagreement with a limit imposed by plasma physics. In Sect. 4 we show that  $\mathcal{D}_{c,s}/\mathcal{D}_{\text{Bohm}} \sim 10^6 - 10^7$  cannot be explained in the framework of any known instability. In Sect. 5 we explore a possible scenario to constrain the maximum energy of particles accelerated in the jet reverse shock, and in Sect. 6 we present our conclusions. Throughout the paper we use cgs units and the cosmology  $H_0 = 71 \text{ km s}^{-1} \text{ Mpc}^{-1}$ ,  $\Omega_0 = 1$  and  $\Lambda_0 = 0.73$ .

## 2 HOTSPOTS

The jet termination region in FR II radiogalaxies is characterised by a double shock structure separated by a contact discontinuity, as sketched in Figure 1. Note however that the contact discontinuity is unstable due to the velocity shear and density contrast in both sides of the discontinuity (e.g. Mizuta et al. 2004). Hotspots are the downstream region of the jet reverse shock, where particles accelerated by the shock emit synchrotron radiation.

**Table 1.** Key features of the argument showing that extreme densities in the jet plasma would be required if the cut-off of the synchrotron spectra were determined by synchrotron cooling, and our new conjecture for an alternative explanation.

Plasma physics	$r_g = \frac{E}{eB}$ $\mathcal{D} = \lambda \frac{c}{3}, \quad \lambda = \frac{r_g^2}{s}$ $c/\omega_{pi} = c/\sqrt{4\pi n_j e^2/\bar{\gamma}_p m_p}$ $s \geq \frac{c}{\omega_{pi}} \Rightarrow \lambda \leq \lambda_{\max} \equiv \frac{r_g^2}{c/\omega_{pi}}$	Larmor radius of particles with energy $E$ and electric charge $e$ in a magnetic field $B$ Diffusion coefficient $\mathcal{D}$ and mean-free path $\lambda$ of particles in a medium with magnetic turbulence of scale length $s$ Ion skin depth in a jet with density $n_j$ and mean energy $\bar{\gamma}_p m_p c^2$ $c/\omega_{pi}$ is the smallest characteristic plasma scale-length <sup>a</sup> (see Sect. 3 and Eq. (15))
Diffusive shock acceleration	$t_{\text{acc}} \sim 20\mathcal{D}/v_{\text{sh}}^2$ $U_e < U_{\text{kin}}$	Acceleration timescale in a parallel shock with velocity $v_{\text{sh}}$ The energy density in non-thermal electrons (see Eq. (20)) cannot be greater than the energy budget $U_{\text{kin}}$ (see Sect. 2 and Eq. (4))
Synchrotron radiation	$\gamma = 4.5 \times 10^{-4} \sqrt{\nu/B}$ $t_{\text{synchr}} = 7.5 \times 10^8 / (\gamma B^2)$	Lorentz factor of electrons emitting synchrotron photons with frequency $\nu$ Synchrotron cooling time
Observations	$\nu_c = 10^{14} - 10^{15} \text{ Hz}$ $E_c = \gamma_c m_e c^2 = \gamma(\nu_c) m_e c^2$	Cut-off of the synchrotron spectrum Non-thermal electrons' maximum energy (see Eqs. (2) and (7))
Reigning paradigm	$t_{\text{acc}}(\gamma_c) = t_{\text{synchr}}(\gamma_c)$ $\lambda_{c,s} \propto v_{\text{sh}}^2 \nu_c^{-1/2} B^{-3/2}$	Synchrotron losses govern where the cut-off is Mean-free path of $\gamma_c$ -electrons (see Sect. 2.2 and Eq. (8))
Combining the above	$n_j > 10^{-5} - 10^{-4} \text{ cm}^{-3}$	A very large jet density is required to be $\lambda_{c,s} \leq \lambda_{\max}$ and $U_e < U_{\text{kin}}$ (see Sect. 3.1 and Table 2)
Our conjecture	$\lambda(E_c, B) \leq r_g(E_c, B_{\text{jd}})$ $E_{\text{nrh}} = E_c \frac{B_{\text{jd}}}{B}$	Condition for particle acceleration in a perpendicular shock with magnetic field $B_{\text{jd}}$ Maximum energy at which non-thermal protons excite non-resonant turbulence (see Sect. 5)

<sup>a</sup> In electron-positron plasmas,  $s$  has to be greater than the electron-skin depth  $c/\omega_{pe}$ , where  $c/\omega_{pe} = \sqrt{m_e/m_p} c/\omega_{pi} \sim 0.02 c/\omega_{pi}$ .

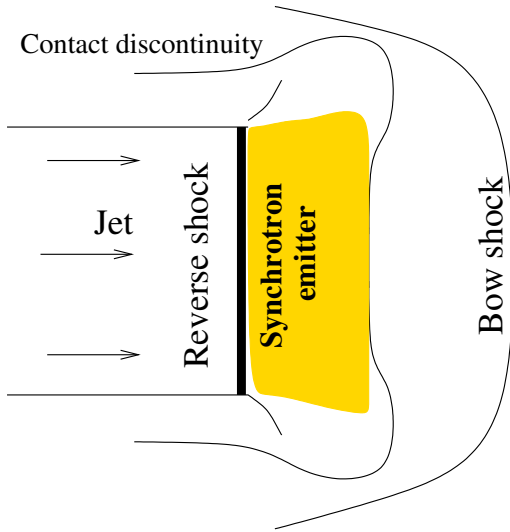


**Figure 1.** Sketch of the standard picture of the jet termination region. Particles are accelerated at the reverse shock, and radiate in the shock downstream region, here labelled “Synchrotron emitter”.

## 2.1 Energy budget

The kinetic energy density of relativistic jets with particles of mass  $m$  and density  $n_j$  and moving with bulk Lorentz factor  $\Gamma_j$  is

$$\frac{U_{\text{kin}}}{\text{erg cm}^{-3}} = 9 \times 10^{-9} \left( \frac{\Gamma_j - 1}{0.06} \right) \left( \frac{n_j}{10^{-4} \text{ cm}^{-3}} \right) \left( \frac{m}{m_p} \right), \quad (4)$$

where  $\Gamma_j = 1.06$  corresponds to a jet velocity  $v_j = c/3$  (Casse & Marcowith 2005; Steenbrugge & Blundell 2008) and  $m_p$  is the proton mass. Even in the case that we do not know

the jet matter composition, we expect that ions (from the jet formation region or from entrainment as the jet propagates) dominate the jet dynamics at the termination region and therefore  $m = m_p$  in Eq. (4). The jet magnetisation parameter is defined as

$$\sigma_j \equiv \frac{U_{\text{mag},j}}{U_{\text{kin}}} \sim 4.4 \times 10^{-6} \left( \frac{B_j}{\mu\text{G}} \right)^2 \left( \frac{\Gamma_j - 1}{0.06} \right)^{-1} \left( \frac{n_j}{10^{-4} \text{ cm}^{-3}} \right)^{-1}, \quad (5)$$

where  $U_{\text{mag},j} = B_j^2/8\pi$  and  $B_j$  is the jet’s magnetic field. The jet (upstream) ram pressure is converted into thermal, non-thermal and magnetic ( $U_{\text{mag}} = 4 \times 10^{-10} (B/100 \mu\text{G})^2 \text{ erg cm}^{-3}$ ) pressure in the shock downstream region with magnetic field  $B$ . The magnetic field in the jet downstream region cannot be greater than

$$\frac{B_{\text{sat}}}{100 \mu\text{G}} = 4.8 \left( \frac{\Gamma_j - 1}{0.06} \right)^{\frac{1}{2}} \left( \frac{n_j}{10^{-4} \text{ cm}^{-3}} \right)^{\frac{1}{2}}, \quad (6)$$

(Meisenheimer & Heavens 1986) which corresponds to the extreme case  $U_{\text{mag}} = U_{\text{kin}}$ . The jet density is unknown in most cases, but  $2 \times 10^{-4} \text{ cm}^{-3}$  is the upper-limit for the primary hotspot in the Western lobe of Cygnus A given the non-detection of radio polarisation (Dreher et al. 1987), and  $6 \times 10^{-5} \text{ cm}^{-3}$  is the upper limit in 3C273 (Meisenheimer & Heavens 1986).

## 2.2 Model to date

Hotspot (radio-to-optical) synchrotron spectra typically show a cut-off at  $\nu_c \gtrsim 10^{14} \text{ Hz}$  (e.g. Meisenheimer et al. 1997; Tavecchio et al. 2005; Zhang et al. 2010; Werner et al. 2012). The traditional assumption is that the maximum energy of non-thermal electrons accelerated at the jet reverse

shock,  $E_c = \gamma_c m_e c^2$ , where

$$\gamma_c \sim 4.5 \times 10^5 \left( \frac{\nu_c}{10^{14} \text{ Hz}} \right)^{\frac{1}{2}} \left( \frac{B}{100 \mu\text{G}} \right)^{-\frac{1}{2}}, \quad (7)$$

is determined by a competition between synchrotron cooling and acceleration timescales (see Table 1). By equating  $t_{\text{synchr}}(\gamma_c) = t_{\text{acc}}(\gamma_c)$ , the diffusion coefficient  $\mathcal{D}_{c,s}$  is given by Eq. (3) and the mean-free path of the  $\gamma_c$ -electrons is

$$\frac{\lambda_{c,s}}{\text{pc}} \sim 25 \left( \frac{v_{\text{sh}}}{c/3} \right)^2 \left( \frac{\nu_c}{10^{14} \text{ Hz}} \right)^{-\frac{1}{2}} \left( \frac{B}{100 \mu\text{G}} \right)^{-\frac{3}{2}}. \quad (8)$$

These electrons radiate half of their energy over a distance

$$\frac{l_c}{\text{kpc}} \sim 0.02 \left( \frac{r}{7} \right)^{-1} \left( \frac{\nu_c}{10^{14} \text{ Hz}} \right)^{-\frac{1}{2}} \left( \frac{B}{100 \mu\text{G}} \right)^{-\frac{1}{2}} \left( \frac{v_{\text{sh}}}{c/3} \right) \quad (9)$$

downstream of the shock, where we have assumed that the velocity of the shocked plasma is  $v_d = v_{\text{sh}}/r$ , being  $4 \lesssim r \lesssim 7$  the adiabatic shock compression factor. Note however that our results are not sensitive to the exact value of  $r$ . The condition  $t_{\text{synchr}}(\gamma_c) = t_{\text{acc}}(\gamma_c)$  implies that the size of the acceleration region is  $L_{\text{acc}} \sim l_c$ .

In some cases, the spectrum is broken at frequency  $\nu_{\text{br}}$ . To avoid misunderstandings between  $\nu_{\text{br}}$  and  $\nu_c$  we show in Fig. 2 two canonical electron and synchrotron spectra: broken (red-dashed lines) and unbroken (green-solid lines). (See e.g. Meisenheimer & Heavens 1986, for a comparison with real spectra.) In sources with enough radio-to-optical data to be able to fit the synchrotron spectrum and measure  $\nu_{\text{br}}$  and  $\nu_c$ , the magnetic field is determined by comparing the synchrotron cooling time at  $\nu_{\text{br}}$  with the timescale  $L/v_d$  to be the particles advected a distance  $L$  from the shock (e.g. Meisenheimer & Heavens 1986):

$$\frac{B}{\mu\text{G}} \sim 354 \left( \frac{r}{7} \right)^{-\frac{2}{3}} \left( \frac{\nu_{\text{br}}}{10 \text{ GHz}} \right)^{-\frac{1}{3}} \left( \frac{v_{\text{sh}}}{c/3} \right)^{\frac{2}{3}} \left( \frac{L}{\text{kpc}} \right)^{-\frac{2}{3}}. \quad (10)$$

Therefore, by replacing  $B$  in Eq. (8), the mean free path of the most energetic electrons accelerated at the shock is

$$\frac{\lambda_{c,s}}{L} \sim 0.05 \left( \frac{r}{7} \right)^{-1} \left( \frac{\nu_{\text{br}}}{\nu_c} \right)^{\frac{1}{2}} \left( \frac{v_{\text{sh}}}{c/3} \right). \quad (11)$$

The main uncertainty is  $L$ , that depends on the angle  $\theta_j$  between the jet and the line of sight through the equation

$$L = \frac{l_{\text{br}} - D \cos \theta_j}{\sin \theta_j}, \quad (12)$$

where  $l_{\text{br}}$  is the observed size at  $\nu_{\text{br}}$  and  $D \sim 2R_j$  is the diameter of the source (when hotspots are modelled as cylinders of thickness  $L$ ). Note that when the jet lies on the plane of the sky,  $\theta_j = 90^\circ$  and  $L = l_{\text{br}}$ .

In the seminal paper of Meisenheimer et al. (1989), using observations at optical, near IR, millimetre and radio bands, hotspots are classified into *high loss* ( $\nu_{\text{br}} \leq 10 \text{ GHz}$ ) and *low loss* ( $\nu_{\text{br}} \gg 10 \text{ GHz}$ ) sources. The latter are characterised by thin emission regions with  $L \sim 0.13$  ( $D/L = 5.85$ ),  $0.06$  ( $D/L = 22$ ), and  $0.07 \text{ kpc}$  ( $D/L = 28.4$ ) in the sources 3C20 West, 3C33 South and 3C111 East, respectively. In these *low loss* sources  $B \sim 0.1 B_{\text{eq}}^1$  and  $\lambda_{c,s} \sim 1\text{--}8 \text{ pc}$ ,

<sup>1</sup> Magnetic fields below the equipartition value  $B_{\text{eq}}$  are also found in hotspots where the X-ray emission is also modelled (e.g.

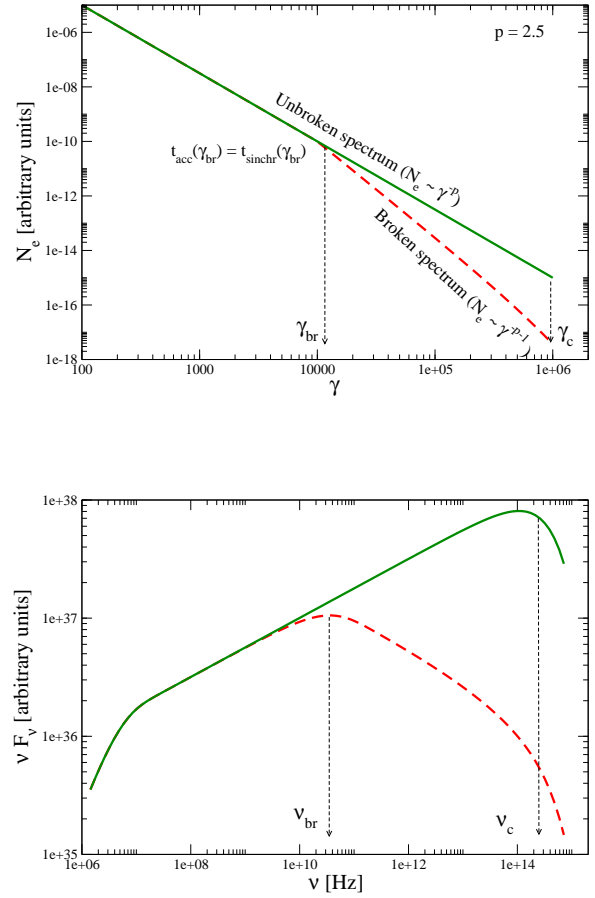


**Figure 2.** *Top:* Non-thermal electron energy distributions for the case where accelerated particles are injected in the shock downstream region following a power-law distribution  $\propto \gamma^{-p}$ , where  $p = 2.5$  (see Sect. 3.1). *Bottom:* Synchrotron spectra. The break  $\gamma_{\text{br}}$  and cut-off  $\gamma_c$  in  $N_e$  correspond to  $\nu_{\text{br}}$  and  $\nu_c$  in the synchrotron spectrum.

where  $B_{\text{eq}}$  is the magnetic field in equipartition with non-thermal particles. The thin (disc-like) emission regions in these hotspots were suggested to be the result of a drastic change in the downstream flow, producing a rapid decay of the magnetic field.

The detection of diffuse IR and optical synchrotron emission on scales larger than  $l_c$  has been interpreted as in-situ re-acceleration (Fermi II) of the non-thermal electrons (Meisenheimer et al. 1997; Prieto et al. 2002; Brunetti et al. 2003). Later on, Mack et al. (2009) presented high spatial resolution observations at near-IR, optical and radio frequencies of low-power radio hotspots, finding that  $\nu_{\text{br}} \sim$

Zhang et al. 2010; Werner et al. 2012). Werner et al. (2012) mentioned that this behaviour is in agreement with De Young (2002), who showed that magnetic field amplification by magnetohydrodynamic turbulence to equipartition values requires timescales greater than the dwell time of the plasma in the hotspots, unless special conditions are imposed.

$\nu_c \sim 10^{14} - 10^{15}$  Hz in all of them (i.e. *low loss* sources). The cooling time of electrons emitting synchrotron radiation at these high frequencies in a magnetic field  $\sim 10 - 100 \mu\text{G}$  (in equipartition with non-thermal electrons and protons) is  $\sim 2 - 5 \times 10^3$  yr and much shorter than the timescales of adiabatic expansion (see Table 5 in Mack et al. (2009)).

In the next section we demonstrate that the maximum energy at which electrons are accelerated cannot be constrained by synchrotron losses, as usually assumed. To demonstrate this, we consider a sample of hotspots that do not show a break in their synchrotron spectra (green-solid lines in Fig. 2), but our arguments are not restricted to these sources.

### 3 REVISING THE SYNCHROTRON CUT-OFF: WHEN OBSERVATIONAL ASTRONOMY MEETS PLASMA PHYSICS

The synchrotron turnover at  $\nu_c \gtrsim 10^{14}$  Hz observed in hotspots of FR II radiogalaxies indicates that the maximum energy of non-thermal electrons accelerated at the jet reverse shock is  $E_c = \gamma_c m_e c^2$ , where  $E_c$  and  $\gamma_c$  are given by Eqs. (2) and (7), respectively. The Larmor radius of these particles is

$$\frac{r_g(\gamma_c)}{\text{cm}} \sim 9 \times 10^{12} \left( \frac{\nu_c}{10^{14} \text{ Hz}} \right)^{0.5} \left( \frac{B}{100 \mu\text{G}} \right)^{-1.5} \quad (13)$$

and the mean-free path is  $\lambda \sim s/\theta^2 \sim r_g^2/s$ , where  $\theta \sim s/r_g$  is the deflection angle of particles interacting with magnetic inhomogeneities of scale length  $s$ . Considering the jet as a hydrogen plasma with electron and proton thermal Lorentz factors  $\bar{\gamma}_e$  and  $\bar{\gamma}_p \sim \Gamma_j$ , respectively, the ion skin depth downstream of the shock is

$$\frac{c}{\omega_{pi}} \sim 8.6 \times 10^8 \sqrt{\Gamma_j} \left[ \left( \frac{r}{7} \right) \left( \frac{n_j}{10^{-4} \text{ cm}^{-3}} \right) \right]^{-\frac{1}{2}} \text{ cm}. \quad (14)$$

The ratio

$$\frac{r_g(\bar{\gamma}_e)}{c/\omega_{pi}} = \left( \frac{\bar{\gamma}_e m_e c^2}{\Gamma_j m_p c^2} \right) \sigma_j^{-\frac{1}{2}} \sim 2 \frac{\bar{\gamma}_e}{\Gamma_j} \left[ \left( \frac{r}{7} \right)^3 \left( \frac{\sigma_j}{10^{-6}} \right) \right]^{-\frac{1}{2}} \quad (15)$$

shows that the thermal electron Larmor radius is generally larger than  $c/\omega_{pi}$  (in the ‘‘hot electrons/cold protons’’ scenario) in which case  $c/\omega_{pi}$  is the smallest characteristic plasma scalelength. Therefore, considering that  $s \geq c/\omega_{pi}$  for suprathermal particles, we find an upper-limit  $\lambda_{\text{max}}$  to the mean-free path of the most energetic electrons accelerated at the jet reverse shock:

$$\lambda_{\text{max}} = \frac{r_g^2(\gamma_c)}{c/\omega_{pi}} \sim 0.02 \left( \frac{\nu_c}{10^{14} \text{ Hz}} \right) \left( \frac{B}{100 \mu\text{G}} \right)^{-3} \left[ \left( \frac{r}{7} \right) \left( \frac{n_j}{10^{-4} \text{ cm}^{-3}} \right) \right]^{\frac{1}{2}} \text{ pc}, \quad (16)$$

independent of the shock velocity  $v_{\text{sh}}$  (see Table 1). Therefore, the maximum diffusion coefficient is given by

$$\frac{\mathcal{D}_{\text{max}}}{\mathcal{D}_{\text{Bohm}}} = \frac{\lambda_{\text{max}}}{r_g(\gamma_c)} = 3.2 \times 10^4 \left( \frac{\nu_c}{10^{14} \text{ Hz}} \right)^{\frac{1}{2}} \left( \frac{B}{100 \mu\text{G}} \right)^{-\frac{3}{2}} \left[ \left( \frac{r}{7} \right) \left( \frac{n_j}{10^{-4} \text{ cm}^{-3}} \right) \right]^{\frac{1}{2}}. \quad (17)$$

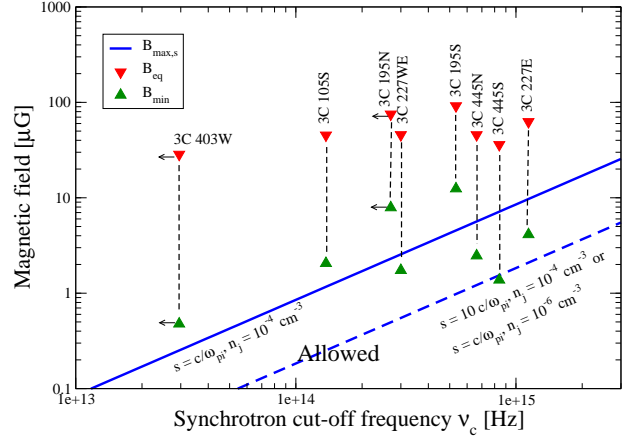


**Figure 3.** Upper limit  $B_{\text{max},s}$  for the magnetic field imposed by the condition  $\lambda_{c,s} \geq \lambda_{\text{max}}$  ( $n_j = 10^{-4} \text{ cm}^{-3}$ : blue-solid line;  $n_j = 10^{-6} \text{ cm}^{-3}$ : blue-dashed line). Triangles indicate the maximum ( $B_{\text{eq}}$ , red triangles down) and minimum ( $B_{\text{min}}$ , green triangles up) field for the sources in Mack et al. (2009); see Table 2.

#### 3.1 Is the maximum energy of non-thermal electrons constrained by synchrotron losses?

If  $\gamma_c$  is determined by a competition between shock acceleration and synchrotron cooling (i.e.  $t_{\text{acc}} = t_{\text{synchr}}$ ), the mean-free path of  $\gamma_c$ -electrons is given by Eq. (8). By comparing  $\lambda_{c,s}$  with the upper-limit  $\lambda_{\text{max}}$ , we find that

$$\frac{\lambda_{c,s}}{\lambda_{\text{max}}} \sim 3 \times 10^4 \left( \frac{v_{\text{sh}}}{c/3} \right)^2 \left( \frac{\nu_c}{10^{14} \text{ Hz}} \right)^{-\frac{3}{2}} \left( \frac{B}{100 \mu\text{G}} \right)^{\frac{3}{2}} \left[ \left( \frac{r}{7} \right) \left( \frac{n_j}{10^{-4} \text{ cm}^{-3}} \right) \right]^{-\frac{1}{2}}. \quad (18)$$

Equivalently, setting  $\lambda_{c,s} \leq \lambda_{\text{max}}$  implies a magnetic field  $B \leq B_{\text{max},s}$ , where

$$\frac{B_{\text{max},s}}{\mu\text{G}} \sim 0.8 \left( \frac{\nu_c}{10^{14} \text{ Hz}} \right) \left( \frac{v_{\text{sh}}}{c/3} \right)^{-\frac{4}{3}} \left[ \left( \frac{r}{7} \right) \left( \frac{n_j}{10^{-4} \text{ cm}^{-3}} \right) \right]^{\frac{1}{3}}. \quad (19)$$

(Note that the same relationship is found by setting  $\mathcal{D}_{c,s} \leq \mathcal{D}_{\text{max}}$ .) In Fig. 3 we plot  $B_{\text{max},s}$  for the cases of  $n_j = 10^{-4}$  (blue-solid line) and  $10^{-6} \text{ cm}^{-3}$  (blue-dashed line). The small values of  $B_{\text{max},s}$  would require a very large energy density in non-thermal electrons in order to explain the synchrotron flux measured at radio-wavelengths. To demonstrate this, we consider the sample of hotspots observed at radio, IR and optical frequencies by Mack et al. (2009), and with a single radio-to-optical spectral index  $\alpha$ , i.e. no spectral break (see Table 2).

Non-thermal electrons follow a power-law energy distribution  $N_e = K_e \gamma^{-p}$  with  $p = 2\alpha + 1$  and minimum Lorentz factor<sup>2</sup> assumed to be  $\gamma_{\text{min}} = 100$ . The electrons energy den-

<sup>2</sup> The value of minimum energy in non-thermal electrons  $E_{\text{min}} = \gamma_{\text{min}} m_e c^2$  cannot be smaller than the energy of the heated plasma downstream of the shock. By equating  $n_j m_p c^2 / 2 = 4 n_j K_B T$ ,

sity is  $U_e \sim K_e \gamma_{\min}^{2-p}/(p-2)$ , where  $K_e$  can be determined from the leptonic emission at a particular frequency. Considering the well resolved emission at  $\nu = 8.4$  GHz, with luminosity  $L_{8.4}$  emitted in a (cylinder-shaped) volume  $V$  (see Table 2),  $U_e$  can be written as

$$\frac{U_e}{\text{erg cm}^{-3}} \sim 10^{-9} \left(\frac{p-2}{0.5}\right)^{-1} \left(\frac{\gamma_{\min}}{100}\right)^{2-p} \left(\frac{\nu}{8.4 \text{ GHz}}\right)^{\frac{p-3}{2}} \left(\frac{L_{8.4}}{10^{41} \text{ erg s}^{-1}}\right) \left(\frac{V}{\text{kpc}^3}\right)^{-1} \left(\frac{B}{100 \mu\text{G}}\right)^{\frac{-p-1}{2}}. \quad (20)$$

The magnetic field is unknown, but we can set the upper and lower-limits. The former corresponds to the magnetic field in equipartition with non-thermal particles. Setting  $U_e(1+a) = B^2/(8\pi)$ , where  $a \geq 0$  takes into account the contribution of non-thermal protons, we find that

$$\frac{B_{\text{eq}}}{\mu\text{G}} \sim 220^{\frac{7.5}{p+5}} \left[ (1+a) \left(\frac{p-2}{0.5}\right)^{-1} \left(\frac{\gamma_{\min}}{100}\right)^{2-p} \left(\frac{\nu}{8.4 \text{ GHz}}\right)^{\frac{p-3}{2}} \left(\frac{L_{8.4}}{10^{41} \text{ erg s}^{-1}}\right) \left(\frac{V}{\text{kpc}^3}\right)^{-1} \right]^{\frac{2}{p+5}}. \quad (21)$$

We calculate  $B_{\text{eq}}$  for all the sources in Mack et al. (2009) assuming  $a = 0$ ; see Table 2 and Fig. 3 (red-triangles down)<sup>3</sup>. Note that  $B_{\text{eq}} \sim 50 \mu\text{G}$  in all the cases, and far greater than  $B_{\text{max},s}$  (blue-solid line), particularly for those cases with  $\nu_c < 10^{15}$  Hz.

### 3.1.1 Minimum value of $B$

In the extreme assumption that the non-thermal electron energy density is  $U_e = U_{\text{kin}}$  (see Eq. (4)), the minimum value of the magnetic field required to emit a luminosity  $L_{8.4}$  at frequency  $\nu$  in a volume  $V$  is

$$\frac{B_{\min}}{\mu\text{G}} \sim 27^{\frac{3.5}{p+1}} \left(\frac{\gamma_{\min}}{100}\right)^{\frac{4-2p}{p+1}} \left(\frac{\nu}{8.4 \text{ GHz}}\right)^{\frac{p-3}{p+1}} \left(\frac{L_{8.4}}{10^{41} \text{ erg s}^{-1}}\right)^{\frac{2}{p+1}} \left[ \left(\frac{\Gamma_j - 1}{0.06}\right) \left(\frac{p-2}{0.5}\right) \left(\frac{V}{\text{kpc}^3}\right) \left(\frac{n_j}{10^{-4} \text{ cm}^{-3}}\right) \right]^{\frac{-2}{p+1}}.$$

We compute  $B_{\min,s}$  for all the sources in Mack et al. (2009); see Table 2 and Fig. 3 (green-triangles up). We can see that  $B_{\min} > B_{\text{max},s}$  (blue-solid line) for those sources with  $\nu_c \lesssim 4 \times 10^{14}$  Hz (3C 105S, 3C 195N, 3C 227WE and 3C 403W) whereas  $B_{\min} < B_{\text{max},s}$  for hotspots with  $\nu_c \gtrsim 4 \times 10^{14}$  Hz (3C 195S, 3C 227E, 3C 445N and 3C 445S). Note however that:

- $n_j \sim 10^{-4} \text{ cm}^{-3}$  is the upper limit found in Cygnus A and 3C475, and therefore we expect values of  $B_{\min}$  greater than those plotted in Fig. 3 when the jet density is smaller than  $10^{-4} \text{ cm}^{-3}$  ( $B_{\min} \propto n_j^{-(p+1)/2}$ ). On the other hand,  $B_{\text{max},s} \propto n_j^{1/3}$  and therefore  $B_{\text{max},s}$  decreases when smaller

where  $K_B$  is the Boltzmann constant and  $T$  is the temperature of the shocked jet, we find that  $K_B T \sim m_p c^2/8 \sim 0.1 \text{ GeV}$  and therefore  $\gamma_{\min}$  has to be greater than 50.

<sup>3</sup> The equipartition field in Eq. (21) is slightly different from the value in Mack et al. (2009) given that we consider a cylinder-shaped volume, instead of an spheroid, and we set  $a = 0$  instead of 1. Note also that Mack et al. (2009) follow the approach of Brunetti et al. (1997) to compute  $B_{\text{eq}}$ .

values of  $n_j$  are considered and the ratio  $B_{\min}/B_{\text{max},s} \propto n_j^{-(p+5/6)}$ . In particular, the blue-dashed line in Fig 3 corresponds to the case of  $n_j = 10^{-6} \text{ cm}^{-3}$  and  $s = c/\omega_{\text{pi}}$ . In such a case, sources 3C 195S, 3C 227E, 3C 445N and 3C 445S move to the regime where  $B_{\min} > B_{\text{max},s}$ . The minimum value of the jet density required to match  $B_{\min} = B_{\text{max},s}$  is listed in Table 2 for all the sources considered in this paper. We can see for instance that the source 3C 195N necessitates  $n_j > 6.5 \times 10^{-4} \text{ cm}^{-3}$  to satisfy the condition  $\lambda_{c,s} < \lambda_{\text{max}}$  and  $U_e < U_{\text{kin}}$ .

- Even when jets in FR galaxies are expected to be perpendicular to the line of sight, a small departure from the plane of the sky (i.e.  $\theta_j < 90^\circ$ ) reduces the size of the shock downstream region (see Eq.(12)). In such a case,  $B_{\min} \propto V^{-2/(p+1)}$  increases whereas  $B_{\text{max},s}$  remains constant. Therefore, the situation is even more strongly ruled out when  $\theta_j < 90^\circ$ .

In the next section we show that even in the case that the extreme conditions discussed before are assumed, the large value of the diffusion coefficient required for  $\gamma_c$  to be determined by synchrotron cooling cannot be explained in any well-established theoretical framework.

## 4 PARTICLE ACCELERATION AND MAGNETIC FIELD AMPLIFICATION

The diffusion coefficient resulting from the assumption that  $\gamma_c$  is determined by synchrotron cooling is very large,  $\mathcal{D}_{c,s}/\mathcal{D}_{\text{Bohm}} \sim 10^6 \cdot 10^7$ , as we show in Eq. (3). For comparison, this is  $\sim 10^3 \cdot 10^4$  times larger than  $\mathcal{D}/\mathcal{D}_{\text{Bohm}}$  for TeV particles diffusing through the Galactic interstellar medium. It is even more extreme when compared with  $\mathcal{D} \sim \mathcal{D}_{\text{Bohm}}$  during diffusive shock acceleration in supernova remnants where the magnetic field is strongly amplified by the non-resonant hybrid (NRH) instability (Bell 2004) and structured on the scale of the cosmic ray (CR) Larmor radius.

In non-relativistic shocks, the condition for the NRH instability to be active is that the upstream magnetic energy density must be less than  $\eta U_{\text{kin}}(v_{\text{sh}}/c)$ , where  $\eta$  is the efficiency with which the available kinetic energy is given to CR (see Sect. 5 and Appendix A). This condition is easily met in hotspots but it may not apply to relativistic shocks. One possible difference is that magnetic field amplification at relativistic shocks might be driven only by mildly relativistic particles since CR spectra at relativistic shocks are relatively steep with the CR energy density dominated by low energy CR. Fully developed magnetic turbulence on the scale of the GeV Larmor radius would naturally scatter TeV particles with  $\mathcal{D}/\mathcal{D}_{\text{Bohm}} \sim 10^3$  since  $\mathcal{D}/\mathcal{D}_{\text{Bohm}} \sim r_g/s$ , as we will see in Sect. 5. However,  $\mathcal{D}/\mathcal{D}_{\text{Bohm}} \sim 10^3$  is not sufficient to explain spectral turnover in the range  $10^{14} - 10^{15}$  Hz (implying  $\mathcal{D}_{c,s}/\mathcal{D}_{\text{Bohm}} \sim 10^6 - 10^7$ ) and the NRH instability must be ruled out if we assume that the turnover is due to synchrotron losses.

In ultra-relativistic shocks in weakly magnetised plasmas ( $\sigma_j < 10^{-3}$ ), the Weibel instability dominates and generates magnetic field on the small scale of the ion collisionless skin depth  $c/\omega_{\text{pi}}$ . Sironi & Spitkovsky (2011) found that the amplified magnetic field has a scalelength of  $\sim 10c/\omega_{\text{pi}}$  but the factor 10 may be due to their shock Lorentz factor

**Table 2.** Physical parameters of the sources considered in this paper. The redshift  $z$ ,  $\nu_c$  and  $\alpha$  are taken from Mack et al. (2009), and  $p = 2\alpha + 1$ . The synchrotron specific luminosity at 8.4 GHz is calculated as  $L_{8.4} = P_{8.4} 10^7 8.4 \times 10^9$ , where  $P_{8.4}$  [W Hz<sup>-1</sup>] is the measured power. The hotspot volume  $V$  is calculated from the angular sizes tabulated in Table 4 of Mack et al. (2009) together with  $P_{8.4}$ .

Source	$z$	$\nu_c$ [10 <sup>14</sup> Hz]	$\alpha$	$p$	$L_{8.4}$ [erg/s]	$V$ [kpc <sup>3</sup> ]	$B_{\text{eq}}$ [ $\mu$ G]	$B_{\text{min}}$ [ $\mu$ G]	$B_{\text{max,s}}$ [ $\mu$ G]	$n_{j,\text{min}}$ [cm <sup>-3</sup> ]
3C 105S	0.089	1.37	0.75	2.5	$1.42 \times 10^{42}$	1205.63	45.27	2.06	1.16	$1.92 \times 10^{-4}$
3C 195N	0.110	<2.70	0.95	2.9	$1.15 \times 10^{41}$	38.12	75.11	7.89	2.30	$6.51 \times 10^{-4}$
3C 195S	0.110	5.34	1.00	3.0	$1.71 \times 10^{41}$	33.58	91.76	12.45	4.55	$3.42 \times 10^{-4}$
3C 227WE	0.086	3.00	0.65	2.3	$3.19 \times 10^{40}$	19.26	45.63	1.74	2.55	$6.78 \times 10^{-5}$
3C 227E	0.086	11.4	0.75	2.5	$7.14 \times 10^{40}$	17.99	62.60	4.12	9.71	$3.96 \times 10^{-5}$
3C 403W	0.059	<0.29	0.55	2.1	$3.95 \times 10^{40}$	167.9	28.46	0.48	0.25	$1.96 \times 10^{-4}$
3C 445N	0.056	6.63	0.85	2.7	$2.18 \times 10^{40}$	29.36	45.60	2.47	5.65	$3.97 \times 10^{-5}$
3C 445S	0.056	8.40	0.80	2.6	$5.04 \times 10^{40}$	139.42	35.94	1.38	7.15	$1.60 \times 10^{-5}$

$\Gamma_j = 15$  which increases  $c/\omega_{\text{pi}}$  by  $\sim \sqrt{\Gamma_j}$  when the relativistic ion mass is allowed for (see Eq. (14)). If we assume fully developed Weibel turbulence with CR scattered by randomly orientated magnetic cells on a scale  $c/\omega_{\text{pi}}$ , the diffusion coefficient is given by  $\mathcal{D}_{\text{max}}/\mathcal{D}_{\text{Bohm}} = r_g(\gamma_c)/(c/\omega_{\text{pi}}) \sim 3 \times 10^4$  as shown in Eq. (17). This value of the diffusion coefficient is large but still much smaller than  $\mathcal{D}_{c,s}/\mathcal{D}_{\text{Bohm}} \sim 10^6\text{-}10^7$  that would be required to explain the spectral turnover at  $\nu_c = 10^{14}$  Hz in a jet with density  $n_j = 10^{-4}$  cm<sup>-3</sup>, at least  $B \leq B_{\text{max,s}}$ . A further difficulty with a Weibel scenario is that post-shock Weibel turbulence decays on a scale of  $\sim 10^3 c/\omega_{\text{pi}} \sim 10^{-5} \sqrt{\Gamma_j} (n_j/10^{-4} \text{cm}^{-3})^{-0.5}$  pc (Sironi & Spitkovsky 2011) which is many orders of magnitude smaller than the size of the hotspot, which is of the order of 10 pc to kpc. We note that the same discrepancy is found in gamma-ray bursts (e.g. Gruzinov & Waxman 1999; Pe'er & Zhang 2006), although it is not completely clear at present how the small-scale magnetic turbulence evolves downstream of the shock (see e.g. Sironi et al. 2015).

Fully developed turbulence with a magnetic field of  $\sim 100$   $\mu$ G cannot be responsible for  $\mathcal{D}_{c,s}/\mathcal{D}_{\text{Bohm}} \sim 10^6\text{-}10^7$  even if its cell size were as small as  $c/\omega_{\text{pi}}$ , as is shown in Fig. 3 and Eq. (17). There remains the possibility that the magnetic field might consist of a long scalelength component with  $B \sim 100$   $\mu$ G with a small-scale perturbation  $\delta B \ll B$ . Magnetic turbulence  $\delta B \ll B$  probably occurs in the Galaxy where CR drift along relatively well-ordered magnetic field lines with weak scattering by Alfvén waves with amplitude  $\delta B$  driven by CR drifts at the order of the Alfvén speed. Under these conditions the CR current is too weak to drive the NRH instability. The Alfvén waves are driven resonantly with a wavelength similar to the CR Larmor radius, and  $\mathcal{D}/\mathcal{D}_{\text{Bohm}} \sim (\delta B/B)^{-2}$  requires fluctuations in the magnetic field as small as  $\delta B/B \sim 10^{-3}$  in order to reach  $\mathcal{D}_{c,s}/\mathcal{D}_{\text{Bohm}} \sim 10^6\text{-}10^7$ . Note however that even in the very weak CR drifts in the interstellar medium  $\mathcal{D}/\mathcal{D}_{\text{Bohm}} \sim 10^3$ . For this scenario to hold for hotspots, a valid theory would need to explain how magnetic field  $B$  could be amplified to  $\sim 100$   $\mu$ G on scales larger than a CR Larmor radius while producing fluctuations  $\delta B$  on a Larmor scale with only  $\delta B/B \sim 10^{-3}$  at a relative amplitude smaller than that found in the Galactic interstellar medium.

Although it is impossible to rule out all possibilities, it appears extremely difficult to construct a scenario in which  $\mathcal{D}_{c,s}/\mathcal{D}_{\text{Bohm}} \sim 10^6\text{-}10^7$ , as required by the supposition that the IR/optical turnover in the synchrotron spectrum is

caused by synchrotron radiation losses. We therefore suggest that the cut-off in the spectrum has a different cause, which we now explore in the next section.

## 5 NON-RESONANT HYBRID INSTABILITIES IN MILDLY RELATIVISTIC SHOCKS

If radiative (synchrotron) losses are not relevant to determining the maximum energy, then this maximum energy must ultimately be determined by the ability to scatter particles downstream of the shock. We explore the possibility that the maximum energy achieved by electrons in the jet reverse shock is constrained by magnetic turbulence generated by low energy CRs in perpendicular shocks.

We consider that the amplified hotspot magnetic field  $B$  is turbulent, and that the large-scale background field downstream of the reverse shock is  $B_{\text{jd}}$  nearly perpendicular to the shock normal because the perpendicular component is compressed and enhanced by a factor of 4 to 7 (i.e.  $B_{\text{jd}} \sim r B_j$ ). In such a case, to accelerate particles up to an energy  $E_c$  via a diffusive mechanism, the mean-free path  $\lambda_c \sim r_g(\gamma_c, B)^2/s$  in the shock downstream region, where  $B$  is a small-scale field, has to be smaller than Larmor radius in  $B_{\text{jd}}$  (Lemoine & Pelletier 2010; Reville & Bell 2014)<sup>4</sup>. The condition  $\lambda_c \lesssim r_g(\gamma_c, B_{\text{jd}})$  is satisfied when the magnetic-turbulence scale-length is

$$s \geq \frac{E_c}{eB} \left( \frac{B_{\text{jd}}}{B} \right) = r_g(\gamma_s, B), \quad (23)$$

where  $r_g(\gamma_s, B)$  is the Larmor radius of protons with energy

$$E_s = E_c \left( \frac{B_{\text{jd}}}{B} \right) = 0.07 E_c \left( \frac{r}{7} \right) \left( \frac{B_j}{\mu\text{G}} \right) \left( \frac{B}{100\mu\text{G}} \right)^{-1} \\ \sim 10 \left( \frac{r}{7} \right) \left( \frac{\nu_c}{10^{14} \text{Hz}} \right)^{\frac{1}{2}} \left( \frac{B_{\text{jd}}}{\mu\text{G}} \right) \left( \frac{B}{100\mu\text{G}} \right)^{-\frac{5}{2}} \text{GeV}, \quad (24)$$

where we take  $B \sim 100$   $\mu$ G and  $B_j \sim \mu$ G as characteristic values. Note that

$$\frac{s}{\text{cm}} > 5 \times 10^{11} \left( \frac{r}{7} \right) \left( \frac{\nu_c}{10^{14} \text{Hz}} \right)^{\frac{1}{2}} \left( \frac{B_{\text{jd}}}{\mu\text{G}} \right) \left( \frac{B}{100\mu\text{G}} \right)^{-\frac{5}{2}} \quad (25)$$

is greater than  $c/\omega_{\text{pi}}$  in Eq. (14), as required. Note however

<sup>4</sup> When the mean-free path of particles in the turbulent field exceeds the Larmor radius in the background compressed field, particles return to helical orbits and diffusion ceases.

that this limit,  $s \gtrsim 500 c/\omega_{\text{pi}}$  for typical values considered in this paper, cannot be fulfilled by Weibel-generated turbulence with scale  $\sim c/\omega_{\text{pi}}$ . Therefore, the maximum energy achieved by electrons in the jet reverse shock,  $E_c$ , cannot be constrained by Weibel instabilities.

Turbulence on a scale greater than  $c/\omega_{\text{pi}}$  may be excited through the non-resonant hybrid (NRH) instability by the diamagnetic drift of CR on either side of the shock. In the simplest form of the NRH instability (Bell 2004, 2005), the CR Larmor radius in the unperturbed background field is much greater than the wavelength of field perturbations and therefore the streaming of CRs carrying the electric current  $j_{\text{cr}}$  is undeflected. The force  $-\vec{j}_{\text{cr}} \times \vec{B}$  acts to expand loops in the magnetic field, and therefore  $B$  increases. This produces an increment in  $-\vec{j}_{\text{cr}} \times \vec{B}$  and generates a positive feedback loop that drives the NRH instability and amplifies the magnetic field. For the diamagnetic drift in the plane of the shock to amplify the magnetic field (see Appendix A) the NRH growth rate has to be sufficient for the instability to grow through  $\sim 10$  e-foldings at the maximum growth rate  $\Gamma_{\text{max}}$  (Bell 2004, 2014) in the time the plasma flows through a distance  $r_{\text{g}}(B_{\text{js}})$  in the downstream region, where  $r_{\text{g}}(B_{\text{js}})$  is the Larmor radius in the ordered field  $B_{\text{js}}$ . That is, the condition  $\Gamma_{\text{max}} r_{\text{g}}(B_{\text{js}})/v_{\text{d}} > 10$  must be satisfied (see Appendix A). If the field is strongly amplified, the instability can be expected to saturate when its characteristic scale grows to the Larmor radius of the CR driving the instability. Thus,  $s$  in Eq. (23) can be expected to match the Larmor radius of the highest energy CR driving the instability. If these CR have an energy  $E_{\text{nrh}}$ , then  $E_{\text{nrh}} \sim E_s$ . From Eq. (24), if  $v_{\text{sh}} \sim c/3$  then CR with energy  $E_{\text{nrh}}$  correspond to mildly supra-thermal protons ( $E_{\text{nrh}} \sim 100 m_p v_{\text{sh}}^2$ ) in the downstream plasma. It is entirely reasonable that protons with this energy should be present in large numbers downstream of the shock and drive the NRH instability.

In order to check that there is enough energy in  $E_{\text{nrh}}$ -protons to excite the non-resonant turbulence, we consider whether the number of e-foldings required to amplify the magnetic field up to the saturation value is of the order of 10 (Bell 2004, 2014). The condition for efficient magnetic field amplification by NRH instabilities is that  $\Gamma_{\text{max}} r_{\text{g}}(B_{\text{js}})/v_{\text{d}} > 10$ , as explained above. This condition leads to

$$\eta > 10 r^{3/2} \sqrt{\sigma_j} \sim 0.04 \left(\frac{r}{7}\right)^{\frac{3}{2}} \left(\frac{B_j}{\mu\text{G}}\right) \left(\frac{\Gamma_j - 1}{0.06}\right)^{-\frac{1}{2}} \left(\frac{n_j}{10^{-4} \text{ cm}^{-3}}\right)^{-\frac{1}{2}} \quad (26)$$

(see Appendix A), where  $\eta \propto P_{\text{CR}}$  is the acceleration efficiency and  $\sigma_j$  is the jet magnetisation parameter defined in Eq. (5). Given that particles accelerated in relativistic shocks follow a power-law energy distribution steeper than the canonical distribution, the CR pressure  $P_{\text{CR}}$  is dominated by low energy particles. Therefore, the condition for NRH instability growth is that the acceleration efficiency of low energy CR has to be  $\eta \sim 0.04$  for characteristic values considered in this paper. Such a value of  $\eta$  is very reasonable. For comparison, CR acceleration in supernova remnants is usually thought to be in the range 10%-50%.

From these estimations we can conclude that NRH instabilities generated by CRs with energies  $\lesssim E_{\text{nrh}}$  can grow fast enough to amplify the jet magnetic field from  $\sim 1$  to 100  $\mu\text{G}$  and accelerate particles up to energies  $\sim E_c$  ob-

served in the hotspots of FR II radiogalaxies. The advantage of magnetic turbulence being generated by CR current is that the amplified magnetic field persists over long distances downstream of the shock, and therefore particles accelerated very near the shock can emit synchrotron radiation far downstream. This framework also applies to hotspots with break in the synchrotron spectrum, and we will explore this situation in depth in a following paper.

## 6 SUMMARY AND CONCLUSIONS

Motivated by the recent realisation of magnetic field damping in the southern hotspot of the radiogalaxy 4C74.26 (Araudo et al. 2015), we have explored in great depth the physical conditions in the hotspots of a larger number of FR II radiogalaxies. In particular, we have investigated the physical mechanism that constraints the maximum energy of particles accelerated at the jet reverse shock.

Based on one observable (the cut-off  $\nu_c$  of the synchrotron spectrum) and one physical requirement ( $s \geq c/\omega_{\text{pi}}$ ) we have found that extreme conditions in the jet plasma would be required for  $\nu_c \sim 10^{14}$ - $10^{15}$  Hz to be determined by synchrotron cooling, as usually assumed. By equating the acceleration and synchrotron cooling timescales, the mean free path of  $\nu_c$ -synchrotron emitting electrons is greater than the maximum value  $r_{\text{g}}^2/(c/\omega_{\text{pi}})$  imposed by plasma physics for reasonable values of the magnetic field and jet density (see Eq. (18)). By considering a sample of 8 hotspots observed with high spatial resolution at optical, IR and radio wavelengths (Mack et al. 2009), we show that unreasonably large values of the jet density would be required (see Table 2) to explain the synchrotron flux at 8.4 GHz when  $E_c$  (maximum energy of non-thermal electrons) is determined by synchrotron cooling (see Fig. 3). The key steps in our argument are outlined in Table 1.

As mentioned in Sect. 4, the structure of the magnetic field downstream of the shock is not completely understood at the moment. Weibel-mediated shocks generate the magnetic field and accelerate particles (e.g. Spitkovsky 2008b; Martins et al. 2009). However, the characteristic scale of Weibel turbulence cannot account for the cut-off of the synchrotron spectrum observed in hotspots because this scale size is too small, nor the large extent of the hotspot synchrotron emission, much larger than the magnetic decay of  $\sim 100c/\omega_{\text{pi}}$  predicted by numerical calculations. A viable alternative is that turbulence is generated by the streaming of CRs with energy  $E_{\text{nrh}} \sim E_c B_{\text{jd}}/B \sim 0.01 E_c$  (see Sect. 5). The amplified magnetic field has a scale-length of the order of the Larmor radius of  $E_{\text{nrh}}$ -protons and persists over long distances downstream of the shock, accounting for the extent of the synchrotron emitting hotspot.

In a future work, we will apply our arguments to the very well known sources Cygnus A and 3C445 for which well resolved and multi-wavelength data are available (e.g. Orienti et al. 2012; Pyrzas et al. 2015). By modelling the particle acceleration and transport downstream the shock we will be able to determine the details of the magnetic field structure downstream of mildly relativistic shocks.

## ACKNOWLEDGEMENTS

The authors would like to thank the referee for a constructive report, and M.A. Prieto for providing useful information about the sources considered in this paper. A.T.A. thanks M. Perucho, W. Potter and L. Sironi for useful discussions about jet physics. The research leading to this article has received funding from the European Research Council under the European Community's Seventh Framework Programme (FP7/2007-2013)/ERC grant agreement no. 247039. We acknowledge support from the UK Science and Technology Facilities Council under grant No. ST/K00106X/1.

## REFERENCES

- Araudo A. T., Bell A. R., Blundell K. M., 2015, *ApJ*, **806**, 243  
 Araudo A. T., Bell A. R., Blundell K. M., 2016, preprint, (arXiv:1602.07896)  
 Bell A. R., 2004, *MNRAS*, **353**, 550  
 Bell A. R., 2005, *MNRAS*, **358**, 181  
 Bell A. R., 2014, *Brazilian Journal of Physics*, **44**, 415  
 Brunetti G., Setti G., Comastri A., 1997, *A&A*, **325**, 898  
 Brunetti G., Mack K.-H., Prieto M. A., Varano S., 2003, *MNRAS*, **345**, L40  
 Casse F., Marcowith A., 2005, *Astroparticle Physics*, **23**, 31  
 De Young D. S., 2002, *New Astron. Rev.*, **46**, 393  
 Dreher J. W., Carilli C. L., Perley R. A., 1987, *ApJ*, **316**, 611  
 Fanaroff B. L., Riley J. M., 1974, *MNRAS*, **167**, 31P  
 Ginzburg V. L., Syrovatskii S. I., 1964, *The Origin of Cosmic Rays*  
 Gruzinov A., Waxman E., 1999, *ApJ*, **511**, 852  
 Hillas A. M., 1984, *ARA&A*, **22**, 425  
 Kirk J. G., Reville B., 2010, *ApJ*, **710**, L16  
 Kotera K., Olinto A. V., 2011, *ARA&A*, **49**, 119  
 Lagage P. O., Cesarsky C. J., 1983, *A&A*, **125**, 249  
 Lemoine M., Pelletier G., 2010, *MNRAS*, **402**, 321  
 Mack K.-H., Prieto M. A., Brunetti G., Orienti M., 2009, *MNRAS*, **392**, 705  
 Martins S. F., Fonseca R. A., Silva L. O., Mori W. B., 2009, *ApJ*, **695**, L189  
 Meisenheimer K., Heavens A. F., 1986, *Nature*, **323**, 419  
 Meisenheimer K., Roser H.-J., Hiltner P. R., Yates M. G., Longair M. S., Chini R., Perley R. A., 1989, *A&A*, **219**, 63  
 Meisenheimer K., Yates M. G., Roser H.-J., 1997, *A&A*, **325**, 57  
 Mizuta A., Yamada S., Takabe H., 2004, *ApJ*, **606**, 804  
 Nagano M., Watson A. A., 2000, *Reviews of Modern Physics*, **72**, 689  
 Norman C. A., Melrose D. B., Achterberg A., 1995, *ApJ*, **454**, 60  
 Orienti M., Prieto M. A., Brunetti G., Mack K.-H., Massaro F., Harris D. E., 2012, *MNRAS*, **419**, 2338  
 Pe'er A., Zhang B., 2006, *ApJ*, **653**, 454  
 Prieto M. A., Brunetti G., Mack K.-H., 2002, *Science*, **298**, 193  
 Pyrzas S., Steenbrugge K. C., Blundell K. M., 2015, *A&A*, **574**, A30  
 Rachen J. P., Biermann P. L., 1993, *A&A*, **272**, 161  
 Reville B., Bell A. R., 2014, *MNRAS*, **439**, 2050  
 Sironi L., Spitkovsky A., 2011, *ApJ*, **726**, 75  
 Sironi L., Spitkovsky A., Arons J., 2013, *ApJ*, **771**, 54  
 Sironi L., Keshet U., Lemoine M., 2015, *Space Sci. Rev.*, **191**, 519  
 Spitkovsky A., 2008a, *ApJ*, **673**, L39  
 Spitkovsky A., 2008b, *ApJ*, **682**, L5  
 Stage M. D., Allen G. E., Houck J. C., Davis J. E., 2006, *Nature Physics*, **2**, 614  
 Stawarz L., Cheung C. C., Harris D. E., Ostrowski M., 2007, *ApJ*, **662**, 213  
 Steenbrugge K. C., Blundell K. M., 2008, *MNRAS*, **388**, 1457  
 Tavecchio F., Cerutti R., Maraschi L., Sambruna R. M., Gambill J. K., Cheung C. C., Urry C. M., 2005, *ApJ*, **630**, 721  
 Werner M. W., Murphy D. W., Livingston J. H., Gorjian V., Jones D. L., Meier D. L., Lawrence C. R., 2012, *ApJ*, **759**, 86  
 Zhang J., Bai J. M., Chen L., Liang E., 2010, *ApJ*, **710**, 1017

## APPENDIX A: CONDITION FOR EFFICIENT NRH INSTABILITY IN HOTSPOTS

As noted in Sect. 5, a condition for effective CR scattering by turbulent magnetic fields amplified by the NRH instability with maximum growth rate  $\Gamma_{\max}$  is that  $\Gamma_{\max} r_g / v_d > 10$  where  $v_d$  is the downstream flow velocity and  $r_g$  is the Larmor radius of the CR driving the instability. The perpendicular component of the magnetic field in the jet is compressed by the shock producing a downstream field that is predominantly perpendicular on the large scale. Drift of CR along the shock surface produces a diamagnetic current that can drive the NRH instability. The CR current  $j_{\text{CR}}$  is perpendicular to both the shock normal and the large scale magnetic field and extends a distance  $\sim r_g$  downstream of the shock. The NRH instability must be driven through many e-foldings during the time  $t_{\text{amp}} \sim r_g / v_d$  during which a fluid element is subject to the diamagnetic current. In this configuration the NRH growth rate is smaller by a numerical factor of order one than in the case of aligned currents and magnetic field (Bell 2005). However,  $\Gamma_{\max} \sim j_{\text{CR}} \sqrt{4\pi / \rho_{\text{jd}}}$  is still a good order-of-magnitude measure of the growth rate, where  $\rho_{\text{jd}} \sim r m_p n_j$  is the density in the shock downstream region. The condition  $\Gamma_{\max} t_{\text{amp}} \sim 10$  provides a good estimate of the time  $t_{\text{amp}}$  for strong non-linear amplification, giving

$$\sqrt{\frac{4\pi}{\rho_{\text{jd}} v_d^2}} \int j_{\text{CR}} dz > 10, \quad (\text{A1})$$

where  $j_{\text{CR}}$  depends on distance  $z$  from the shock. From the momentum equation the downstream CR pressure  $P_{\text{CR}}$  must be balanced by the magnetic force:  $\int j_{\text{CR}} B_{\text{jd}} dz \approx P_{\text{CR}}$  giving the condition

$$\sqrt{\frac{4\pi}{\rho_{\text{jd}} v_d^2}} \left( \frac{P_{\text{CR}}}{B_{\text{jd}}} \right) > 10, \quad (\text{A2})$$

or equivalently

$$\eta = \frac{P_{\text{CR}}}{\rho_{\text{jd}} v_d^2} > 10 \left( \frac{B_{\text{jd}}^2 / 4\pi}{\rho_{\text{jd}} v_d^2} \right)^{1/2} = 10 r^{3/2} \sqrt{\sigma_j} \quad (\text{A3})$$

where  $\eta = P_{\text{CR}} / \rho v_d^2$  is the CR acceleration efficiency, as quoted in Sect. 5. Equation A3 is thus the condition for efficient NRH instability in jet reverse shocks.

This paper has been typeset from a  $\text{\TeX}/\text{\LaTeX}$  file prepared by the author.